https://doi.org/10.5194/hess-2020-149
Preprint. Discussion started: 14 April 2020

Hydrology and Earth System Sciences
Discussions

Rivers in the sky, flooding on the ground

Monica Ionita[1], Viorica Nagavciuc[1,2] and Bin Guan[3,4]

[1] Alfred Wegener Institute for Polar and Marine Research, Bremerhaven, 27570, Germany
[2] Faculty of Forestry, Ștefan cel Mare University, Suceava, 720229, Romania
[3] Joint Institute for Regional Earth System Science and Engineering, University of California, Los Angeles, CA, USA,
[4] Jet Propulsion Laboratory, California Institute of Technology, Pasadena, CA, USA

Correspondence to: Monica Ionita (Monica.Ionita@awi.de)

Abstract. The role of the large scale atmospheric circulation and atmospheric rivers (ARs) in producing extreme flooding and heavy rainfall events in the lower part of Rhine River catchment area is examined in this study. Analysis of the largest 10 floods in the lower Rhine, between 1817 – 2015, indicate that all these extreme flood peaks have been preceded up to 7 days in advance by intense moisture transport from the tropical North Atlantic basin, in the form of narrow bands, also know as atmospheric rivers. The influence of ARs on the Rhine River flood events is done via the prevailing large-scale atmospheric circulation. Most of the ARs associated with these flood events are embedded in the trailing fronts of the extratropical cyclones. The typical large scale atmospheric circulation leading to heavy rainfall and flooding in the lower Rhine is characterized by a low pressure center south of Greenland which migrates towards Europe and a stable high pressure center over the northern part of Africa and southern part of Europe. The days preceding the flood peaks, lower (upper) level convergence (divergence) is observed over the analyzed region, which is an indication of strong vertical motions and heavy rainfall. The results presented in this study offer new insights regarding the importance of tropical moisture transport as driver of extreme flooding in the lower part of Rhine River catchment area and we show for the first time that ARs are an useful tool for the identification of potential damaging floods inland Europe.

1 Introduction

The intensity and frequency of precipitation extremes and floods have increased over the last decades in many parts of the world (Blöschl et al., 2015; Stadtherr et al., 2016). As a consequence, an increase in the flood hazard and its associated damages, has become a major concern both for society and economy. In terms of economical losses, floods are the most widespread hazard at European level (Barredo, 2009; Paprotny et al., 2018). Throughout the last decades Europe has been affected by a large number of heavy rainfall events corroborated with damaging floods. Among the most costliest and damaging floods, at European level, we have: the 1993 and 1995 winter floods in France, Germany, Netherlands and Belgium (Chbab, 1995; Disse and Engel, 2001; Engel, 1997; Finkl et al., 1995); the 2000, 2007 and 2014 floods in U.K. (Kelman, 2001; Muchan et al., 2015; Posthumus et al., 2009; Stevens et al., 2016); the 2002 and 2013 damaging floods in the Elbe river catchment area (Ionita et al., 2015; Ulbrich et al., 2003a, 2003b); the 2005 floods in the eastern part of Europe (Barredo, 2007; Ionita, 2015) and the 2010 floods in central part of Europe (Bissolli et al., 2011), among others. These recent floods, recorded in different parts of the European continent, have shown that coping with floods is not a trivial thing and for a better management and improvement of flood predictions it is necessary to improve our understanding of the underlying mechanisms of these extreme events. Taking into account the fact that climate change is expected to lead to an intensification of the hydrological cycle and in particular the hydrological extremes (Allan et al., 2014; O'Gorman and Schneider, 2009) it is imperative to properly understand the

https://doi.org/10.5194/hess-2020-149
Preprint. Discussion started: 14 April 2020


Hydrology and Earth System Sciences
Discussions

relationship between heavy rainfall events and floods and the prevailing large-scale atmospheric circulation on scales from planetary to mesoscale, in order to be able to provide skillful forecasts of upcoming floods in terms of time of occurrence, location and magnitude.

Flood risk management decisions and flood forecasting depends strongly on our understanding of the large scale drivers of hydrological variability (DeFlorio et al., 2019; Guan and Waliser, 2019a; Lavers et al., 2014). The timing, magnitude and duration of floods and heavy rainfall events depends on the hydroclimatic variability on different time scales ranging from hourly, daily, seasonal to interannual. This variability is connected to the large scale moisture transport on the entire atmospheric column, which in turn is controlled by different large scale teleconnection patterns such as the North Atlantic Oscillation (NAO), the Pacific North American Oscillation (PNA) and El Niño-Southern Oscillation (ENSO) (Guan et al., 2013; Paltan et al., 2017). Apart from these pre-defined large-scale teleconnection patterns, regional and local climates also modulate the water vapor transport, in the form of transient, narrow and elongated corridors, also known as atmospheric rivers (ARs) (Zhu and Newell, 1994; Guan and Waliser, 2019a; Ralph et al., 2018; Shields et al., 2018). ARs are responsible for ~90% of the poleward vertically integrated water vapor transport outside of the tropics and at any time there are at least 3 to 5 ARs around the globe (Guan and Waliser, 2015; Zhu and Newell, 1998). Their horizontal dimensions can be up to several thousands km long with an average width of ~ 500km (Ralph et al., 2004; Ralph and Dettinger, 2011).

Different studies have linked the occurrence of ARs to extreme rainfall and flooding in different parts of the world, although they also provide beneficial rain and snow to many arid/semi-arid areas. For example, in California, ARs contribute to 30 – 50% of the river flow (Dettinger, 2011) and they supply on average ~30% of the total precipitation in the west coast of U.S and Europe (Lavers and Villarini, 2013a). On the other hand, heavy floods in California and Washington states have been linked to ARs occurrence (Neiman et al., 2011; Ralph et al., 2006), and similar results were later found in other west-coast areas. In a recent study, Little et al. (2019) have shown that ARs are a major contributor to extreme snowfall and ablation in the Southern Alps of New Zeeland. At European level ARs have been found to significantly influence heavy rainfall events over the Iberian Peninsula (Brands et al., 2017; Ramos et al., 2015), U.K. (Lavers et al., 2011; Lavers and Villarini, 2015), Norway (Benedict et al., 2019) and France (Lu et al., 2013). Lavers et al. (2011) have shown that U.K. extreme floods and precipitation are mainly driven by ARs, while Lu et al. (2013) related the extreme floods in the western part of France in January 1995 with tropical moisture exports in the form of ARs.

All the aforementioned studies, at European level, were conducted over coastal regions, where ARs make landfall, thus contributing substantially to extreme rainfall events and floods over these regions. Nevertheless, for the European mainland there are limited studies which show a direct link between ARs occurrence and heavy rainfall events and flooding. For example, Paltan et al. (2017) have shown that 50% of the Rhine river floods can be related to ARs, but their study took into account all floods peaks which are exceeded 10% of the time, over the period 1979 - 2010. In this study we want to explore the relationship between the 10 highest flood peaks (in terms of magnitude) in the lower part of Rhine river catchment area and the tropical moisture transport and large-scale atmospheric circulation over the last 180 years, including the lead/lag relationship between the timing of flood peaks and the occurrence of AR conditions which has not been the focus of previous studies on AR-related flooding.

https://doi.org/10.5194/hess-2020-149
Preprint. Discussion started: 14 April 2020

The objectives of this study are to (i) analyze from a hydrological point of view three of the most damaging winter floods (1925/26, 1993 and 1995) in the lower part of Rhine River catchment area; (ii) analyze the large-scale circulation preceding these extreme flood events; (iii) link the flood peaks with the occurrence of ARs and (iv) use a cohesive long-term data sets (e.g. reanalysis products) to analyze the common drivers of 10 of the highest flood peaks (in terms of magnitude) recorded at Köln gauging station, situated in the lower Rhine.

The outline of the study is as follows. The basic features of the Rhine River catchment area are described in Section 2, while the data and methods are described in Section 3. The hydrometeorological situation in relationship with the most damaging floods is given in Section 4. The main conclusions of the paper are presented in Section 5.

2 Catchment area

Rhine River ranks the 9th among the Eurasian rivers, having a total length of ~1250 km, a drainage area of ~185260 km^2 and an average streamflow of 2300 m^3/s. The catchment area of Rhine River covers 9 countries (Germany, Austria, Switzerland, Belgium, Luxembourg, Lichtenstein, Italy, France and the Netherlands) (Figure 1), while the river itself provides services for inland waterway transportation, drinking water, power generation, agriculture, tourism and urban sanitation (Uehlinger et al., 2009). The Rhine is Europe's most important inland waterway, transporting almost 200 million tons per year (approximately two-thirds of the European inland waterway volume) (Meißner et al., 2017).

The Rhine river has a complex runoff regime, with a summer maximum on the Alpine, High and Upper Rhine, and a winter maximum due to the influence of the largest tributaries, the Main and Moselle, on the Middle and Lower Rhine. Extreme flood events in the Rhine region can be divided into two types according to the hydrometeorological causes: winter or spring floods, which are triggered by warm air intrusions with corresponding snow melt in flatlands and low mountain ranges and summer floods, which are fed by large-scale heavy rain or long-lasting repeated precipitation episodes (in connection with late snowmelt / glacier runoff in the Alps). Extreme flood events often do not affect the entire Rhine, but either the Alpine, High and Upper Rhine (mostly in summer) or Middle and Lower Rhine (mostly in winter / spring).

The major tributaries of Rhine river, on the German side are: Neckar, Main and Moselle. All the tributaries are characterized by a pluvial regime, with the mean runoff reaching the highest values in the winter months and the minimum in August- September. Throughout the 20th century, flood peaks show an upward trend in the Alpine and pre-Alpine Rhine basin (Belz et al., 2007). In the Middle and Lower Rhine, extreme floods due to enhanced rainfall sometimes combined with snowmelt, have increased in intensity, especially during the winter months, in the second part of the 20th century (Belz et al., 2007). The increasing trend in the flood peaks, in the Middle and Lower Rhine basin, is largely due to the contribution from the Moselle River where flood waves with peaks up to 4200 m^3/scan occur in winter months (annual mean average discharge at Cochem gauging station = 313 m^3/s). An overall increase in the winter precipitation in the catchments of the lower Rhine tributaries, has caused an increase of ~10% of the mean discharge at Lobith gauging station during the 20th century.

https://doi.org/10.5194/hess-2020-149
Preprint. Discussion started: 14 April 2020

Hydrology and Earth System Sciences
Discussions

3 Data and methods

The main variable analyzed in this study is the daily streamflow data at Köln gauging station situated in the lower part of the Rhein catchment area (Figure 1). The daily streamflow data was provided by the German Hydrological Institute (www.bfg.de). For the large-scale atmospheric circulation, we have used the sea level pressure (SLP), zonal and meridional wind, specific humidity and surface pressure from the 20th Century Reanalysis data V3 (Slivinski et al., 2019). The 20th Century Reanalysis data V3 uses a state-of-the-art data assimilation system and surface pressure observations, it has 64 vertical levels and 80 ensemble members. The output of this reanalysis product is a 4D global atmospheric dataset spanning the period 1836 to 2015. The resolution of the data set is ~1° x 1°. The 20CRv3 has several improvements compared to the previous version 2c, allowing an improved representation of extreme events (Slivinski et al., 2019).

The vertically integrated water vapor transport (IVT) (Peixoto and Oort, 1992) is calculated through zonal wind (u), meridional wind (v) and specific humidity (q), from the 20th Century Reanalysis v3 data set. IVT vectors for latitude (ϕ) and longitude (λ) are defined as follows:

$$\vec{Q}(\lambda,\phi,t) = Q_\lambda \vec{i} + Q_\phi \vec{j}$$

Where zonal (Q_λ) and meridional (Q_Φ) components of Q are given by:

$$Q_\lambda = \int_{1000}^{300} qu \frac{dp}{g}$$

$$Q_\phi = \int_{1000}^{300} qv \frac{dp}{g}$$

For each vertical layer and each grid-point we calculate the product between the daily values of horizontal wind and specific humidity (q). The result is multiplied with the pressure thickness of the layer they represent and divided by gravity. The ARs are identified using the vertically integrated water vapour transport (IVT) between the 1000 and 300 hPa levels. The methodology used in this study to define an AR is based on the global detection algorithm of Guan and Waliser (2015). We consider an AR if the IVT exceeds an intensity threshold (e.g. the local 85th percentile), if it has a minimum value of 100 kg*m^{-1}*s^{-1} and a length of at least 2000 km, among other considerations detailed in Guan and Waliser (2015). Performance of this AR detection algorithm has been validated against dropsonde observations over the north-eastern Pacific (Guan et al., 2017), and results based on this global algorithm were found to agree well with algorithms independently developed for three specific regions (Guan and Waliser, 2015).

To identify the flood events, we extracted, from the daily streamflow time series at Köln gauging station, the top ten daily streamflow values over the period 1817 – 2019 . We have compared our flood events with the ones from the information platform of the German Hydrological Institute (http://undine.bafg.de/rhein/rheingebiet.html). We have restricted our analysis just over the winter months (November – March), due to the fact that summer floods tend to be produced by different mechanisms (e.g. convective precipitation). For the top 10 winter flood events over the lower Rhine River basin (Table 1), we have extracted also daily precipitation and daily mean air temperature at Trier weather station, which is situated on the main course of Moselle River, one of the most important tributaries of Rhine River. We choose Trier station due to its length (1907 – 2019) and due to the fact that most of the floods on the lower basin of Rhine river are mainly influenced by the input from the Moselle

https://doi.org/10.5194/hess-2020-149
Preprint. Discussion started: 14 April 2020


Hydrology and Earth System Sciences
Discussions

river (Figure 1). The daily precipitation and daily mean air temperature data were extracted from the ftp server of the German Weather Service (ftp://opendata.dwd.de/climate_environment/CDC/). The gridded precipitation data was extracted from the EOBS-v20e data set (Cornes et al., 2018).

4 Results

4.1 Hydrometeorological situation - 1925/26

The last week of November 1925 was characterized by heavy snowfall in the western part of Germany and the lower areas of the Rhine River basin (Soldan, 1927). After a short period of dry and cold days, at the beginning of the second week of December it began to thaw, until mid-December. In parts of the Rhine area, heavy snowfall corroborated with extremely low temperatures were recorded over the period 12 – 18th of December 1925 (Figure S1 and Figure S2). After this period of heavy snowfall and low temperatures, warm and humid air masses penetrated from the south-west on the 26th of December. The warm and humid air slid onto the cold air between the mountains of the Rhine region and caused extremely high rainfall in the large parts of the Rhine catchment area between 27th until 29th of December 1925 (Figure S3). From the 27th until 31st of December heavy rainfall affected large parts of the Moselle's catchment area and the lower part of Rhine River basin. The highest rainfall amount, at Trier station, was recorded on the 27th od December (27mm) (Figure 2a). The cumulated rainfall amount over the period 27 – 31 December was 92.5mm. Overall, in December 1925 the total rainfall amount over the lower part of Rhine Rivers basin was on average more than double compared to the climatological mean (Figure S4a). These extreme rainfall events in the last week of December 1925, were driven by a dipole-like structure in the SLP filed with a deep low pressure system (960 hPa) centered south of Greenland and a high pressure system (1025 hPa) centered over the northern part of Africa (Figure 3a). This dipole-like structure started to develop on the 25th of December and persisted until the 31st of December, slightly shifting its centers (Figure 3). This circulation structure led to a pronounced south-westerly air flow over France and western part of Germany, associated with a narrow band of atmospheric moisture extending from the U.S coast up to central part of Europe. The narrow band of moisture was particular active on the 27th, 28th, 29th and 30th of December (Figure 3c, 3d, 3e and 3f), leading to heavy rainfall over northern part of France and western part of Germany (Figure S3). As this band of moisture ascended in the warm sector of the extra-tropical cyclone and was forced to rise over the mountain areas in the Moselle catchment area (southern Vosges Mountains in France, and Hunsrück and Eifel Mountains in Germany), heavy rainfall was forced and thus the high flood peaks some days later in the lower part of Rhine River basin. At Trier gauging station, the flood peak reached its third highest value (3600 m^3/s) on the 31st of December 1925.

Looking more into detail into the dynamic fields of specific moisture during the days with heavy rainfall events, one can identify a distant source of moisture. During the days of rainfall events, recorded at Trier station, a long and narrow band of moisture at 900 hPa level is transported from the sub-tropical latitudes, passing the North Atlantic Ocean and reaching the western part of Europe (Figure 4 – left column, shaded areas). This narrow band of moisture is transported by a southwestern wind, at 900 hPa level, above 20m/s (Figure 4 – left column, vectors). This combination of wind and specific moisture, concentrated in such narrow bands suggests the

https://doi.org/10.5194/hess-2020-149
Preprint. Discussion started: 14 April 2020


Hydrology and Earth System Sciences
Discussions

presence of an AR, in agreement with the results obtained by using the AR tracking algorithm of Guan and Waliser (2015) (Figure 3).

In order to further analyze the dynamical drivers of extreme flood events we computed the divergence filed for the upper (300 hPa) and lower (900 hPa) levels wind speed. The wind speed and its associated divergence/convergence at the 900 (300) hPa level are shown in Figure 4 (Figure S5). The upper level analysis (Figure S5) indicates the presence of an upper level jet branch, shifted southwards and stretching from the central North Atlantic basin until the central part of Europe and an area with upper level divergence over our analyzed region (contour lines in Figure S5), which is an indicator of deep convection (Hoskins et al., 1978; Krichak et al., 2014). In addition, at lower levels, we can observe an intense low-level jet is present with a similar orientation as the upper level jet (Figure 4 – right column) over the analyzed region. The upper level divergence and lower level convergence over our analyzed region, are an indication of strong vertical motions and heavy rainfall (Hoskins et al., 1978). The days characterized by rainfall episodes (e.g. 27 – 31.12.1925 – Figure 2a) are all associated with a southward shift of the polar front, convergence over the catchment area (dashed lines in Figure 4b, 4d, 4f and 4h) and enhanced moisture transport in narrow band stretching from the tropical Atlantic until our analyzed region (Figure 4a, 4c, 4e and 4g).

From a hydrological perspective, the thaw that started in the second week of December 1925 brought the first flood peaks in the Rhine River and its tributaries (especially the Neckar and Mosel), which peaked in the middle of the month (Figure 2b). The subsequent frost period reduced the water flow, before the renewed thaw caused rising peaks again in the third week of December. Over this period of time, most of the Rhine River tributaries (e.g. the Aare, Murg, Kinzig, Neckar, Lahn) and especially the Moselle brought relatively large volumes of water to the Rhine (Soldan, 1927). This caused the flood peaks in the Middle and Lower Rhine to rise abruptly. The subsequent brief cold snap caused the water levels to drop again from 23rd of December, before the abrupt weather change on 26th of December, which led to the outstanding flood event. The rapid ascent of the Rhine began on the 27th of December. On the Upper Rhine, the flood peak of the Ill river merged with that of the Rhine on the 30th of December (Soldan, 1927). The water of the Moselle reached the Rhine on early January 1. Dike breaks occurred above Köln and at Neuss. In the Prussian Rhine province, more than 28.000 houses and 2,500 businesses were flooded, and more than 13.500 apartments had to be cleared. The most severely damaged cities were Köln and Koblenz with 72.000 and 14.000 people affected. Agricultural damage was also significant as 74.000 hectares of land were under water. Arable crops and crop stocks were destroyed and gravel and sand were deposited on the cultivated areas. The damage to hydraulic engineering systems on the Rhine, Mosel and Ruhr was put at 376.000 DM. The damage to the traffic facilities outside the rivers was rather small given the size of the flood. The total damage was given as 100 million DM for the Prussian Rhine region (Soldan, 1927).

4.2 Hydrometeorological situation - 1993

November 1993 and the first week of December 1993 were characterized by relatively reduced amounts of rainfall over Rhine River catchment area (Bornefeld, 1994). Between 8th to 24th of December, the general weather situation was characterized by several Atlantic low pressure systems (heavy storm with hurricane gusts on December 9) and a stable high pressure system in front of the North African continent, which led too frequent rainfall, sometimes heavy rain over the northern part of France and western part of Germany (Deutscher

https://doi.org/10.5194/hess-2020-149
Preprint. Discussion started: 14 April 2020


Hydrology and Earth System Sciences
Discussions

Wetterdienst, 1994). The maximum amount of precipitation, at Trier station, was recorded on the 20th of December 1993 (33.3mm) (Figure 5a). Overall, in the period from 8th to 20th of December 1993, in the catchment areas of Neckar, Nahe and Mosel, as well as in large parts of the central Upper Rhine and central Middle Rhine, more than double of the long-term December precipitation, was recorded (Figure S4b). The extratropical cyclones in the North Atlantic persisted several days pushing a narrow band of moisture towards central Europe (Figure 6). High rates of IVT (up to 800 kg m^{-1} s^{-1}) were recorded from the 18th until 21st of December (Figure 6b, 6c and 6d). At the same time, warm, humid air entered the Rhine area, which led to an extraordinary increase in temperature (Figure 5a). After a rainless 18th of December, the 19th and 20th of December were characterized by heavy rainfall events over most of Rhine's River catchment area (Figure 5a). As in the case of the 1925/26 flood event, the days characterized by heavy rainfall over our analyzed region (Figure S6) are associated with a narrow band of specific humidity at 900 hPa level, stretching from the sun-tropical North Atlantic basin until the central part of Europe, strong winds directed towards the western part of Europe (Figure 7a and 7c) and lower (upper) level converge (divergence) (Figure 7b and 7d, Figure S7). This large-scale pattern is favorable of strong vertical motions and heavy rainfall over our analyzed region.

The precipitation in the first half of December 1993 caused the soil to become saturated with water, so that the subsequent rain had an immediate drainage effect. However, a noteworthy flood wave only developed in the Rhine from the inflow of the Neckar, which led to a significant flood and reached its peak water level on December 22 at the Rockenau level (Engel et al., 1994). The highest flow at the Kaub level dates to December 23rd. An extraordinarily flood peak developed in the Moselle, and the highest daily streamflow of the century was recorded at the Cochem gauging station on the 22nd of December (4020 m^3/s). This flood peak in the Moselle merged with the Rhine on December 23, leading to one of the largest known flood waves of the Rhine downstream of Koblenz (Figure 5b). The combined flood peak passed through Andernach on 23rd of December 1993 and reached Köln gauging station on 24th of December (10600 m^3/s) (Figure 5b), where the flood protection wall of the old town was flooded for about 70 hours, and Rees and Emmerich cities on the following day.

The Christmas flood in the Rhine area caused several human losses and required evacuations in many cities. In Baden-Württemberg (Neckar area), Rhineland-Palatinate and North Rhine-Westphalia high building damage occurred. In Koblenz, almost a quarter of the built-up area of the city was flooded, while 10.000 inhabitants and ~ 4.000 houses were directly affected by the flood. In North Rhine-Westphalia, the number of damaged households was considerable, especially in Königswinter, Bonn and especially in Köln. In Köln, over 4500 households had a direct flood damage and another 9000 households suffered damage from increased groundwater. The damage to the federal shipping routes was estimated to be ~DM 12 million. Due to the flooding, the shipping had to be completely stopped on Neckar and Saar for 9 days, on the Mosel 12 days and on the Rhine from Koblenz to the Dutch border for 7 days. The lost transport revenues were estimated at over 50 million DM. A total of approximately DM 1 billion was damaged in the Rhine region (Münchener Rückversicherungs-Gesellschaft, 1999).

4.3 Hydrometeorological situation - 1995

After local heavy rain in the higher low mountain regions at the end of December 1994, several periods of precipitation in January 1995 brought heavy rainfall to the entire Rhine region (Engel, 1999). The cold spell in

https://doi.org/10.5194/hess-2020-149
Preprint. Discussion started: 14 April 2020


Hydrology and Earth System Sciences
Discussions

the first week of January 1995 (Figure 8a) led to snow fall in the middle part of Rhine River. In the Alpine region there were almost 100 cm of snow recorded at the end of the first week of January 1995. In the second week of January 1995, a north-westerly flow led to daily showers on top of the accumulated snow (Engel, 1999). Thus, the rainfall corroborated with the snow melt, due the temperature increase, led to small flood peaks along the Rhine and its tributaries (Figure 8b). The situation become exceptional starting with the 22nd of January 1995. The rainfall episodes began on the evening of the 21st of January and last ~30 hours. Berus meteorological station recorded 60.1mm of rainfall in 24h, which represent 90% of the monthly normal for January (Ulbrich and Fink, 1995). The extreme rainfall episode was triggered by a frontal system which deepened into a low pressure system over the western part of Europe. On the 22nd of January 1995, Trier meteorological station recorded the highest daily precipitation amount (49.6mm) over the last 70 years for the month of January. This event led to an increase in the water levels of Moselle river to a flood peak of 2880m^3/s at Trier station and 3410 m^3/s at Cochem gauging station, on the 23rd of January 1995 (Figure 8b). On the 25th of January 1995, another exceptional rainfall event was recorded, with values up to 55mm in 24 hours over large area in the Moselle and Rhine catchment areas (Figure S8). This event was triggered by an AR event, with a magnitude of ~600 $kg*m^{-1}*s^{-1}$ (Figure 9b) and a westerly large-scale atmospheric circulation characterized by a deep low pressure system over Scandinavia and a high pressure system over northern part of Africa. Between 26th to 29th of January 1995, small frontal waves driven by the low pressure system south of Greenland (Figure 9c-f) led to more rainfall episodes (Figure 8a) over Moselle's catchment area and large parts of Rhine River catchment area (Figure S8). These frontal systems were corroborated with ARs stretching from the sub-tropical North Atlantic basin and bringing moisture to the western part of Europe (Figure 9e and 9f).

The prevailing large-scale atmospheric circulation, during the days characterized by enhanced rainfall over large area of Rhine's catchment area (Figure S8), featured narrow bands of moisture transport from the sub-tropical North Atlantic basin towards the western part of Europe (Figure 10a, 10c, 10e and 10g) and enhanced lower level convergence over central part of Europe (Figure 10b, 10d, 10f and 10h). The upper level large-scale atmospheric circulation was characterized by divergence over Rhine's catchment area (Figure S9), ascending motions and heavy rainfall (Figure S8).

As a result of the repeated rainfall episodes, the catchment area in the Middle and Lower Rhine as well as the tributaries Main, Nahe, Mosel and Sieg saw a steep increase in daily streamflow (Engel, 1999). The water inflow from the Main and Nahe rivers resulted in a significant increase in the flood wave at the Mainz and Kaub gauges, where the Christmas flooding from 1993 was exceeded. On 30th of January 1995, after the flooding of the Moselle began, the flood peaks of the Rhine reached 10700 m^3/s at Köln gauging station (the second highest daily streamflow recorded over a period of 200 years). Due to the flood inflow of the Sieg, the flood peak at Köln gauging station was further increased, reaching with a water level 6 cm higher than during the Christmas flood in 1993 (Engel, 1999). At the Rees gauging station the peak of the flood wave was 11300 m^3/s and was above the Christmas flood in 1993 (10600 m^3/s) and only just below the highest known flood peak in January 1926 (11700 m^3/s). Overall, the extreme floods of January 1995 were mainly triggered by long lasting rainfall episodes driver by frontal systems from the North Atlantic basin, a high frequency of AR events and intense moisture transport from the sub-tropical North Atlantic basin until the western part of Europe, as well as a southward shift of the polar front and upper (lower) level divergence (convergence) over the analyzed region.

https://doi.org/10.5194/hess-2020-149
Preprint. Discussion started: 14 April 2020

The 1995 floods had huge consequences both for society and economy in Germany and the Netherlands. In numerous cities and towns on the Rhine and the tributaries, streets and houses were flooded, power outages and damage to the infrastructure occurred and 5 people were killed (Münchener Rückversicherungs-Gesellschaft, 1999). The total monetary damage in the German Rhine catchment area estimated to be ~ DM 550 million. Due to the exceeding of the highest navigable water levels, shipping had to be temporarily suspended on individual sections of the and the monetary losses for the shipping related companies was ~ DM 50 million. For the Köln city alone, the damage was around DM 65 million (half as much as in the 1993 Christmas flood) and 4000 people were directly affected by the floods. In the Netherlands, at least 4 people were killed and ~250,000 people had to be evacuated because of dike breaches and extensive flooding of polders and large parts of cities were submerged between 30 January and 1 February 1995 –from the Limburg region south of Nijmegen and from Zeeland, around Rotterdam, Europe's largest port (Münchener Rückversicherungs-Gesellschaft, 1999).

4.4 Composite events

The crucial role that ARs have in preceding extreme flooding in the lower part of Rhine river catchment area is highlighted also by analyzing the IVT, SLP and the AR origin with different time lags (0 – 7 days) for the 10 highest flood peaks measured at Köln gauging station. The occurrence date and the magnitude of each flood peak are shown in Table 1. The composite of all flood peaks shows that all of them are preceded up to 7 days by a plum of moisture, in the shape of an AR, accompanied by a deep low pressure center over the British Isles and a high pressure center over the Iberian Peninsula (Figure 11). The moisture is transported towards France and the western part of Germany by a south-westerly wind (Figure 11). By visual inspection the ARs associated with heavy winter floods in the lower part of the Rhine River basin have an elongated shape, thus confirming the AR geometrical criterion of being at least 2000km long and less than 1000 km wide (Ralph et al., 2004; Neiman et al., 2008).

Snapshots of the evolution of the AR axis, indicating the development and propagation of the AR prior to the occurrence date of the top 10 flood peaks, over the last 180 years, are shown in Figure 12. The evolution of ARs for the different snapshots demonstrate further the importance of moisture transport from the North Atlantic Ocean in producing damaging floods in the lower part of Rhine river basin. In all cases the moisture transport is directed towards the north-western part of France penetrating until the western part of Germany. The axis of the ARs is strongly influenced by the dipole-like structure in the SLP field, with a deep low over the central part of the North Atlantic and a high pressure system over the northern part of Africa and Iberian Peninsula. For all the 10 analyzed cases there was at least one AR preceding the flood peak with a lag varying between 2 to 7 days.

5. Conclusions

The variability of European precipitation, in winter, is strongly affected by enhanced moisture transport from the sub-tropical North Atlantic basin. Overall, ARs are responsible for ~20-30% of all recorded precipitation in regions situated in the western part of Europe (mainly France and Iberian Peninsula) (Gimeno et al., 2016). While ARs are essential ingredients in producing heavy rainfall events and flooding over the coastal areas of the European continent (e.g. Portugal, Spain, France, Norway) little is known about their influence on the precipitation and flood events inland Europe (Gimeno et al., 2016). Although there have been numerous studies

https://doi.org/10.5194/hess-2020-149
Preprint. Discussion started: 14 April 2020


Hydrology and Earth System Sciences
Discussions

linking ARs with floods and heavy precipitation, over large parts of the world (Benedict et al., 2019; Dettinger, 2011; Guan and Waliser, 2019b; Lavers et al., 2011; Lavers and Villarini, 2013b; Marengo et al., 2016; Neiman et al., 2008; Paltan et al., 2017; Vázquez et al., 2017, among others) this is the first study in which ARs are linked with specific events of extreme flooding inland Europe, more specific over the lower part of Rhine catchment area, which is one of the biggest rivers in Europe. The lower part of Rhine catchment area is dominated by winter floods, which are often caused by westerly, southwesterly and north-westerly large-scale circulation types (Beurton and Thieken, 2009). In this study we have shown that extreme floods, in winter, occur predominantly during mild and wet episodes associated with a southwards shift of the polar front and frontal systems moving from the North Atlantic basin towards Europe, corroborated with intense moisture transport from the sub-tropical North Atlantic basin until the western part of Europe. Although the mechanism behind each individual extreme flood is rather different, heavy snowfall followed by thawing and/or just extreme rainfall events, for the analyzed cases there is one thing in common: the heavy snowfall and/or rainfall are driven by intense moisture transport from the Atlantic basin, towards northern part of France and western part of Germany, in narrow and long bands, which in contact with high mountain regions over the Moselle catchment area and parts of Rhine catchment area lead to extreme flooding. The typical large-scale synoptic circulation leading to heavy rainfall events and extreme flooding, in the lower part of Rhine's catchment area, is characterized by a zonal flow circulation with a deep and mobile low pressure center south of Greenland, which migrates towards the northern part of Europe, and a high pressure system over the northern part of Africa and southern part of Europe. The strong pole to equator temperature gradient, in winter, results in an enhanced baroclinic zone and storm tracks affecting the western part of Europe. The extratropical cyclones, associated with the extreme flooding events over western part of Europe, including the lower catchment area of Rhine river, grow in these baroclinic zones which also contain the ARs that make landfall over the European land mass (Lavers and Villarini, 2013b). The influence of ARs on the Rhine River flood events is done via the prevailing large-scale atmospheric circulation and most of the ARs associated with these flood events are embedded in the trailing fronts of the extratropical cyclones.

One of the most interesting finding of this study is the fact that the extreme floods are preceded, especially 4-5 days in advance (Figure 12), by intense moisture transport from the sub-tropical Atlantic, in the form of ARs. This time lag between the ARs occurrence and the flood peak, in the lower part of the catchment area of Rhine river, can be used as a potential predictor for the upcoming floods in the lower part of Rhine catchment area. Overall, the North Atlantic ARs are projected to increase both in magnitude and frequency, implying a greater risk of extreme rainfall and flooding (Lavers et al., 2013), thus more studies are needed to test if also smaller flood peak are associated with intense moisture transport and their potential predictability.

This study adds new understanding of the meteorological processes leading to the occurrence of extreme rainfall events and flooding in the central part of Europe. Identifying ARs as a potential contributor to floods in the lower part of Rhine River catchment area, thus inland Europe, indicates the need for further studies to better understand the drivers of hydrometeorological extremes over different parts of Europe, thus allowing for a better assessment of flood risk.

https://doi.org/10.5194/hess-2020-149
Preprint. Discussion started: 14 April 2020

Hydrology and Earth System Sciences
Discussions

Acknowledgements. This study was promoted by Helmholtz funding through the Polar Regions and Coasts in the Changing Earth System (PACES) program of the AWI. Funding by the AWI Strategy Fund Project - PalEX and by the Helmholtz Climate Initiative - REKLIM are gratefully acknowledged.

Author contributions. MI designed the study and wrote the paper. VN and BG helped with the writing of the paper and interpret the results.

Competing interests. The authors declare that they have no conflict of interest.

https://doi.org/10.5194/hess-2020-149
Preprint. Discussion started: 14 April 2020

Hydrology and Earth System Sciences
Discussions

References

Allan, R. P., Liu, C., Zahn, M., Lavers, D. A., Koukouvagias, E. and Bodas-Salcedo, A.: Physically Consistent Responses of the Global Atmospheric Hydrological Cycle in Models and Observations, Surv. Geophys., 35(3), 533–552, doi:10.1007/s10712-012-9213-z, 2014.

Barredo, J. I.: Major flood disasters in Europe: 1950-2005, Nat. Hazards, 42(1), 125–148, doi:10.1007/s11069-006-9065-2, 2007.

Barredo, J. I.: Normalised flood losses in Europe: 1970-2006, Nat. Hazards Earth Syst. Sci., 9(1), 97–104, doi:10.5194/nhess-9-97-2009, 2009.

Belz, J. U., Brahmer, G., Buiteveld, H., Engel, H., Grabher, R., Hodel, H., Krahe, P., Lammersen, R., Larina, M., Mendel, H., Meuser, A., Plonka, B., Pfister, L. and Vuuren, W. Van: Das Abflussregime des Rheins und seiner Nebenflüsse Analyse, Veränderungen, Trends. CHR report No. I-22., 2007.

Benedict, I., Ødemark, K., Nipen, T. and Moore, R.: Large-scale flow patterns associated with extreme precipitation and atmospheric rivers over Norway, Mon. Weather Rev., 147(4), 1415–1428, doi:10.1175/MWR-D-18-0362.1, 2019.

Beurton, S. and Thieken, A. H.: Seasonality of floods in Germany, Hydrol. Sci. J., 54(1), 62–76, doi:10.1623/hysj.54.1.62, 2009.

Bissolli, P., Friedrich, K., Rapp, J. and Ziese, M.: Flooding in eastern central Europe in May 2010 - Reasons, evolution and climatological assessment, Weather, 66(6), 147–153, doi:10.1002/wea.759, 2011.

Blöschl, G., Gaál, L., Hall, J., Kiss, A., Komma, J., Nester, T., Parajka, J., Perdigão, R. A. P., Plavcová, L., Rogger, M., Salinas, J. L. and Viglione, A.: Increasing river floods: fiction or reality?, Wiley Interdiscip. Rev. Water, 2(4), 329–344, doi:10.1002/wat2.1079, 2015.

Bornefeld, L.: Das Weihnachtshochwasser 1993 des Rheins. Ein Beitrag des Staatlichen Amtes für Wasser- und Abfallwirtschaft Düsseldorf, Düsseldorf., 1994.

Brands, S., Gutiérrez, J. M. and San-Martín, D.: Twentieth-century atmospheric river activity along the west coasts of Europe and North America: algorithm formulation, reanalysis uncertainty and links to atmospheric circulation patterns, Clim. Dyn., 48(9–10), 2771–2795, doi:10.1007/s00382-016-3095-6, 2017.

Chbab, E. H.: How extreme were the 1995 flood waves on the rivers Rhine and Meuse?, Phys. Chem. Earth, 20(5–6), 455–458, doi:10.1016/S0079-1946(96)00005-5, 1995.

Cornes, R. C., van der Schrier, G., van den Besselaar, E. J. M. and Jones, P. D.: An Ensemble Version of the E-OBS Temperature and Precipitation Data Sets, J. Geophys. Res. Atmos., 123(17), 9391–9409, doi:10.1029/2017JD028200, 2018.

DeFlorio, M. J., Waliser, D. E., Guan, B., Ralph, F. M. and Vitart, F.: Global evaluation of atmospheric river subseasonal prediction skill, Clim. Dyn., 52(5–6), 3039–3060, doi:10.1007/s00382-018-4309-x, 2019.

Dettinger, M.: Climate change, atmospheric rivers, and floods in California - a multimodel analysis of storm frequency and magnitude changes, J. Am. Water Resour. Assoc., 47(3), 514–523, doi:10.1111/j.1752-1688.2011.00546.x, 2011.

Deutscher Wetterdienst: Dezember 1993. -Monatlicher Witterungsbericht, Offenbach., 1994.

Disse, M. and Engel, H.: Flood events in the Rhine basin: Genesis, influences and mitigation, Nat. Hazards, 23(2–3), 271–290, doi:10.1023/A:1011142402374, 2001.

Engel, H.: The flood events of 1993/1994 and 1995 in the Rhine River basin, IAHS-AISH Publ., (239), 21–32, 1997.

Engel, H.: Eine Hochwasserperiode im Rheingebiet - Extremereignisse zwischen Dez. 1993 und Febr. 1995., Lelystad., 1999.

Engel, H., Busch, N., Wilke, K., Krahe, P., Mendel, H.-G., Giebel, H. and Zieger, C.: Das Hochwasser 1993/94 im Rheingebiet., 1994.

Fick, S. E. and Hijmans, R. J.: WorldClim 2: new 1-km spatial resolution climate surfaces for global land areas, Int. J. Climatol., 37(12), 4302–4315, doi:10.1002/joc.5086, 2017.

https://doi.org/10.5194/hess-2020-149
Preprint. Discussion started: 14 April 2020

Finkl, A., Ulbrichl, U. and Engel, H.: Germany, , (January), 2–7, 1995.

Gimeno, L., Dominguez, F., Nieto, R., Trigo, R., Drumond, A., Reason, C. J. C., Taschetto, A. S., Ramos, A. M., Kumar, R. and Marengo, J.: Major Mechanisms of Atmospheric Moisture Transport and Their Role in Extreme Precipitation Events, Annu. Rev. Environ. Resour., 41(1), 117–141, doi:10.1146/annurev-environ-110615-085558, 2016.

Guan, B. and Waliser, D. E.: Detection of atmospheric rivers: Evaluation and application of an algorithm for global studies, J. Geophys. Res. Atmos., 120(24), 12514–12535, doi:10.1002/2015JD024257, 2015.

Guan, B. and Waliser, D. E.: Tracking Atmospheric Rivers Globally: Spatial Distributions and Temporal Evolution of Life Cycle Characteristics, J. Geophys. Res. Atmos., 124(23), 12523–12552, doi:10.1029/2019JD031205, 2019a.

Guan, B. and Waliser, D. E.: Tracking Atmospheric Rivers Globally: Spatial Distributions and Temporal Evolution of Life Cycle Characteristics, J. Geophys. Res. Atmos., 124(23), 12523–12552, doi:10.1029/2019JD031205, 2019b.

Guan, B., Molotch, N. P., Waliser, D. E., Fetzer, E. J. and Neiman, P. J.: The 2010/2011 snow season in California's Sierra Nevada: Role of atmospheric rivers and modes of large-scale variability, Water Resour. Res., 49(10), 6731–6743, doi:10.1002/wrcr.20537, 2013.

Guan, B., Waliser, D. E. and Ralph, F. M.: An Intercomparison between Reanalysis and Dropsonde Observations of the Total Water Vapor Transport in Individual Atmospheric Rivers, J. Hydrometeorol., 19(2), 321–337, doi:10.1175/JHM-D-17-0114.1, 2017.

Hoskins, B. J., Draghici, I. and Davies, H. C.: A new look at the ω-equation, Q. J. R. Meteorol. Soc., 104(439), 31–38, doi:10.1002/qj.49710443903, 1978.

Ionita, M.: Interannual summer streamflow variability over Romania and its connection to large-scale atmospheric circulation, Int. J. Climatol., 35(14), 4186–4196, 2015.

Ionita, M., Dima, M., Lohmann, G., Scholz, P. and Rimbu, N.: Predicting the June 2013 European Flooding Based on Precipitation, Soil Moisture, and Sea Level Pressure, J. Hydrometeorol., 16(2), 598–614, doi:10.1175/JHM-D-14-0156.1, 2015.

Kelman, I.: The autumn 2000 floods in England and flood management, Weather, 56(10), 346–360, doi:10.1002/j.1477-8696.2001.tb06507.x, 2001.

Krichak, S. O., Breitgand, J. S., Gualdi, S. and Feldstein, S. B.: Teleconnection–extreme precipitation relationships over the Mediterranean region, Theor. Appl. Climatol., 117(3), 679–692, doi:10.1007/s00704-013-1036-4, 2014.

Lavers, D. A. and Villarini, G.: Atmospheric rivers and flooding over the central United States, J. Clim., 26(20), 7829–7836, doi:10.1175/JCLI-D-13-00212.1, 2013a.

Lavers, D. A. and Villarini, G.: The nexus between atmospheric rivers and extreme precipitation across Europe, Geophys. Res. Lett., 40(12), 3259–3264, doi:10.1002/grl.50636, 2013b.

Lavers, D. A. and Villarini, G.: The contribution of atmospheric rivers to precipitation in Europe and the United States, J. Hydrol., 522, 382–390, doi:10.1016/j.jhydrol.2014.12.010, 2015.

Lavers, D. A., Allan, R. P., Wood, E. F., Villarini, G., Brayshaw, D. J. and Wade, A. J.: Winter floods in Britain are connected to atmospheric rivers, Geophys. Res. Lett., 38(23), 1–8, doi:10.1029/2011GL049783, 2011.

Lavers, D. A., Allan, R. P., Villarini, G., Lloyd-Hughes, B., Brayshaw, D. J. and Wade, A. J.: Future changes in atmospheric rivers and their implications for winter flooding in Britain, Environ. Res. Lett., 8(3), 34010, doi:10.1088/1748-9326/8/3/034010, 2013.

Lavers, D. A., Pappenberger, F. and Zsoter, E.: Extending medium-range predictability of extreme hydrological events in Europe, Nat. Commun., 5, doi:10.1038/ncomms6382, 2014.

Little, K., Kingston, D. G., Cullen, N. J. and Gibson, P. B.: The Role of Atmospheric Rivers for Extreme Ablation and Snowfall Events in the Southern Alps of New Zealand, Geophys. Res. Lett., 46(5), 2761–2771, doi:10.1029/2018GL081669, 2019.

Lu, M., Lall, U., Schwartz, A. and Kwon, H.: Precipitation predictability associated with tropical moisture exports and circulation patterns for a major flood in France in 1995, Water Resour. Res., 49(10), 6381–6392, doi:10.1002/wrcr.20512,

https://doi.org/10.5194/hess-2020-149
Preprint. Discussion started: 14 April 2020

2013.

Marengo, J., Gimeno, L., Dominguez, F., Nieto, R., Trigo, R., Drumond, A., Reason, C. J. C. and Kumar, R.: Major Mechanisms of Atmospheric Moisture Transport and their Role in Extreme Precipitation Events Major Mechanisms of Atmospheric Moisture Transport and their Role in Extreme Precipitation Events, , 3(June), 38231, doi:10.1146/annurev-environ-110615-085558, 2016.

Meißner, D., Klein, B. and Ionita, M.: Development of a monthly to seasonal forecast framework tailored to inland waterway transport in central Europe, Hydrol. Earth Syst. Sci., 21(12), doi:10.5194/hess-21-6401-2017, 2017.

Muchan, K., Lewis, M., Hannaford, J. and Parry, S.: The winter storms of 2013/2014 in the UK: hydrological responses and impacts, Weather, 70(2), 55–61, doi:10.1002/wea.2469, 2015.

Münchener Rückversicherungs-Gesellschaft: Naturkatastrophen in Deutschland - Schadenerfahrungen und Schadenpotentiale, München., 1999.

Neiman, P. J., Ralph, F. M., Wick, G. A., Lundquist, J. D. and Dettinger, M. D.: Meteorological characteristics and overland precipitation impacts of atmospheric rivers affecting the West coast of North America based on eight years of SSM/I satellite observations, J. Hydrometeorol., 9(1), 22–47, doi:10.1175/2007JHM855.1, 2008.

Neiman, P. J., Schick, L. J., Martin Ralph, F., Hughes, M. and Wick, G. A.: Flooding in western washington: The connection to atmospheric rivers, J. Hydrometeorol., 12(6), 1337–1358, doi:10.1175/2011JHM1358.1, 2011.

O'Gorman, P. A. and Schneider, T.: The physical basis for increases in precipitation extremes in simulations of 21st-century climate change, Proc. Natl. Acad. Sci. U. S. A., 106(35), 14773–14777, doi:10.1073/pnas.0907610106, 2009.

Paltan, H., Waliser, D., Lim, W. H., Guan, B., Yamazaki, D., Pant, R. and Dadson, S.: Global Floods and Water Availability Driven by Atmospheric Rivers, Geophys. Res. Lett., 44(20), 10,387-10,395, doi:10.1002/2017GL074882, 2017.

Paprotny, D., Sebastian, A., Morales-Nápoles, O. and Jonkman, S. N.: Trends in flood losses in Europe over the past 150 years, Nat. Commun., 9(1), doi:10.1038/s41467-018-04253-1, 2018.

Peixoto, J. P. and Oort, A. H.: Physics of climate, Springer Berlin Heidelberg., 1992.

Posthumus, H., Morris, J., Hess, T. M., Neville, D., Phillips, E. and Baylis, A.: Impacts of the summer 2007 floods on agriculture in England, J. Flood Risk Manag., 2(3), 182–189, doi:10.1111/j.1753-318X.2009.01031.x, 2009.

Ralph, F. M. and Dettinger, M. D.: Storms, floods, and the science of atmospheric rivers, Eos, Trans. Am. Geophys. Union, 92(32), 265–266, doi:10.1029/2011EO320001, 2011.

Ralph, F. M., Neiman, P. J. and Wick, G. A.: Satellite and CALJET Aircraft Observations of Atmospheric Rivers over the Eastern North Pacific Ocean during the Winter of 1997/98, Mon. Weather Rev., 132(7), 1721–1745, doi:10.1175/1520-0493(2004)132<1721:SACAOO>2.0.CO;2, 2004.

Ralph, F. M., Neiman, P. J., Wick, G. A., Gutman, S. I., Dettinger, M. D., Cayan, D. R. and White, A. B.: Flooding on California's Russian River: Role of atmospheric rivers, Geophys. Res. Lett., 33(13), doi:10.1029/2006GL026689, 2006.

Ralph, F. M., Dettinger, M. C. L. D., Cairns, M. M., Galarneau, T. J. and Eylander, J.: Defining "Atmospheric river" : How the glossary of meteorology helped resolve a debate, Bull. Am. Meteorol. Soc., 99(4), 837–839, doi:10.1175/BAMS-D-17-0157.1, 2018.

Ramos, A. M., Trigo, R. M., Liberato, M. L. R. and Tomé, R.: Daily precipitation extreme events in the Iberian Peninsula and its association with atmospheric rivers, J. Hydrometeorol., 16(2), 579–597, doi:10.1175/JHM-D-14-0103.1, 2015.

Shields, C. A., Rutz, J. J., Leung, L. Y., Martin Ralph, F., Wehner, M., Kawzenuk, B., Lora, J. M., McClenny, E., Osborne, T., Payne, A. E., Ullrich, P., Gershunov, A., Goldenson, N., Guan, B., Qian, Y., Ramos, A. M., Sarangi, C., Sellars, S., Gorodetskaya, I., Kashinath, K., Kurlin, V., Mahoney, K., Muszynski, G., Pierce, R., Subramanian, A. C., Tome, R., Waliser, D., Walton, D., Wick, G., Wilson, A., Lavers, D., Prabhat, Collow, A., Krishnan, H., Magnusdottir, G. and Nguyen, P.: Atmospheric River Tracking Method Intercomparison Project (ARTMIP): Project goals and experimental design, Geosci. Model Dev., 11(6), 2455–2474, doi:10.5194/gmd-11-2455-2018, 2018.

Slivinski, L. C., Compo, G. P., Whitaker, J. S., Sardeshmukh, P. D., Giese, B. S., McColl, C., Allan, R., Yin, X., Vose, R., Titchner, H., Kennedy, J., Spencer, L. J., Ashcroft, L., Brönnimann, S., Brunet, M., Camuffo, D., Cornes, R., Cram, T. A., Crouthamel, R., Domínguez-Castro, F., Freeman, J. E., Gergis, J., Hawkins, E., Jones, P. D., Jourdain, S., Kaplan, A.,

https://doi.org/10.5194/hess-2020-149
Preprint. Discussion started: 14 April 2020

Kubota, H., Blancq, F. Le, Lee, T.-C., Lorrey, A., Luterbacher, J., Maugeri, M., Mock, C. J., Moore, G. W. K., Przybylak, R., Pudmenzky, C., Reason, C., Slonosky, V. C., Smith, C. A., Tinz, B., Trewin, B., Valente, M. A., Wang, X. L., Wilkinson, C., Wood, K. and Wyszyński, P.: Towards a more reliable historical reanalysis: Improvements for version 3 of the Twentieth Century Reanalysis system, Q. J. R. Meteorol. Soc., 145(724), 2876–2908, doi:10.1002/qj.3598, 2019.

Soldan, W.: Die großen Schadenhochwässer der letzten Jahre und ihre Ursachen, Zentralblatt der Bauverwaltung, 47(19/20), 233–237, 1927.

Stadtherr, L., Coumou, D., Petoukhov, V., Petri, S. and Rahmstorf, S.: Record Balkan floods of 2014 linked to planetary wave resonance, Sci. Adv., 2(4), e1501428, doi:10.1126/sciadv.1501428, 2016.

Stevens, A. J., Clarke, D. and Nicholls, R. J.: Trends in reported flooding in the UK: 1884–2013, Hydrol. Sci. J., 61(1), 50–63, doi:10.1080/02626667.2014.950581, 2016.

Uehlinger, U., Arndt, H., Wantzen, K. M. and Leuven, R. S. E. W.: Chapter 6 - The Rhine River Basin, in Rivers of Europe, edited by K. Tockner, U. Uehlinger, and C. T. Robinson, pp. 199–245, Academic Press, London., 2009.

Ulbrich, U. and Fink, A.: The January 1995 flood in Germany: Meteorological versus hydrological causes, Phys. Chem. Earth, 20(5–6), 439–444, doi:10.1016/S0079-1946(96)00002-X, 1995.

Ulbrich, U., Brücher, T., Fink, A. H., Leckebusch, G. C., Krüger, A. and Pinto, J. G.: The central European floods of August 2002: Part 1 – Rainfall periods and flood development, Weather, 58(10), 371–377, doi:10.1256/wea.61.03A, 2003a.

Ulbrich, U., Brücher, T., Fink, A. H., Leckebusch, G. C., Krüger, A. and Pinto, J. G.: The central European floods of August 2002: Part 2 –Synoptic causes and considerations with respect to climatic change, Weather, 58(11), 434–442, doi:10.1256/wea.61.03B, 2003b.

Vázquez, M., Pereira, K., Nieto, R. and Gimeno, L.: The origin of moisture feeding up Atmospheric Rivers over the Arctic, , 1(November), 4829, doi:10.3390/chycle-2017-04829, 2017.

Zhu, Y. and Newell, R. E.: Atmospheric rivers and bombs, Geophys. Res. Lett., 21(18), 1999–2002, doi:10.1029/94GL01710, 1994.

Zhu, Y. and Newell, R. E.: A Proposed Algorithm for Moisture Fluxes from Atmospheric Rivers, Mon. Weather Rev., 126(3), 725–735, doi:10.1175/1520-0493(1998)126<0725:APAFMF>2.0.CO;2, 1998.

https://doi.org/10.5194/hess-2020-149
Preprint. Discussion started: 14 April 2020

Hydrology and Earth System Sciences
Discussions

605 **Table 1**. Date of occurrence and magnitude of the ten flood events recorded at Köln gauging station used in this study.

Date	Magnitude
31.03.1845	9.800 m^3/s
5.02.1850	9.710 m^3/s
29.11.1882	10.200 m^3/s
16.01.1920	10.700 m^3/s
1.01.1926	10.900 m^3/s
2.01.1948	9.890 m^3/s
25.02.1970	9.690 m^3/s
29.03.1988	9.550 m^3/s
24.12.1993	10.600 m^3/s
31.01.1995	10.700 m^3/s

610

615

620

625

630

635

https://doi.org/10.5194/hess-2020-149
Preprint. Discussion started: 14 April 2020

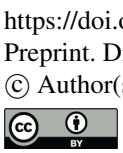

Hydrology and Earth System Sciences
Discussions
Open Access
EGU

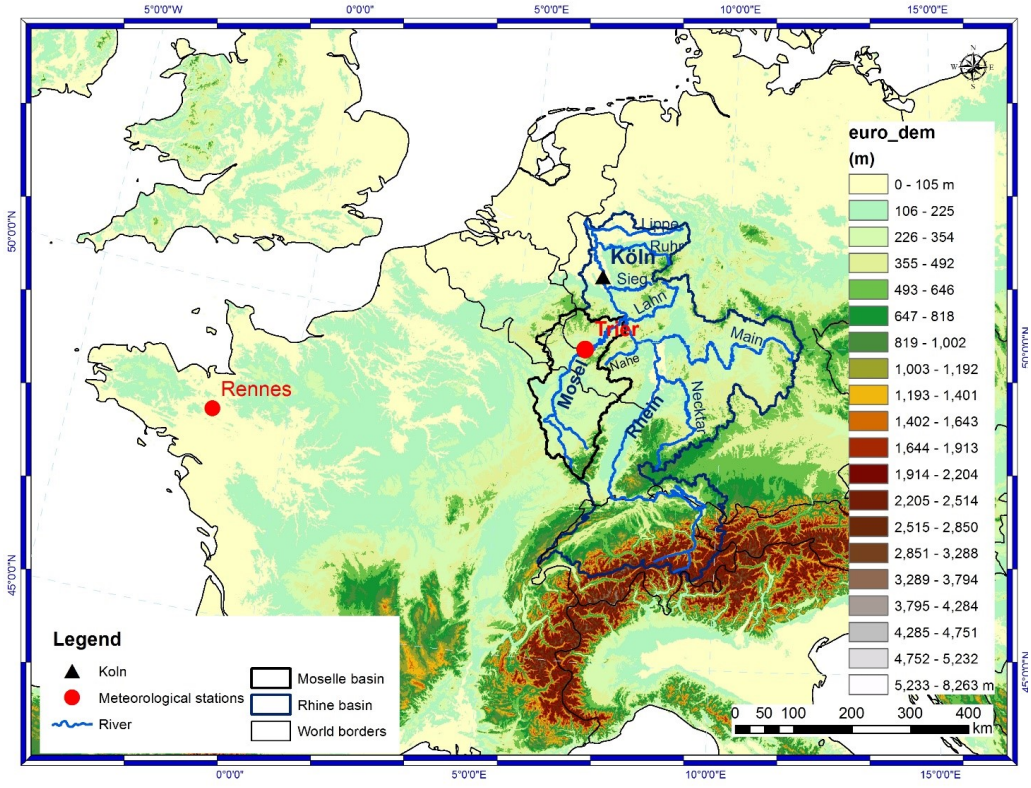

Figure 1. Rhine River catchment area (black contour) and the location of Trier meteorological station and Köln gauging station. The digital elevation model data was extracted from the WorldClim 2 dataset (Fick and Hijmans, 2017).

640

645

650

655

https://doi.org/10.5194/hess-2020-149
Preprint. Discussion started: 14 April 2020

Hydrology and Earth System Sciences
Discussions

a)

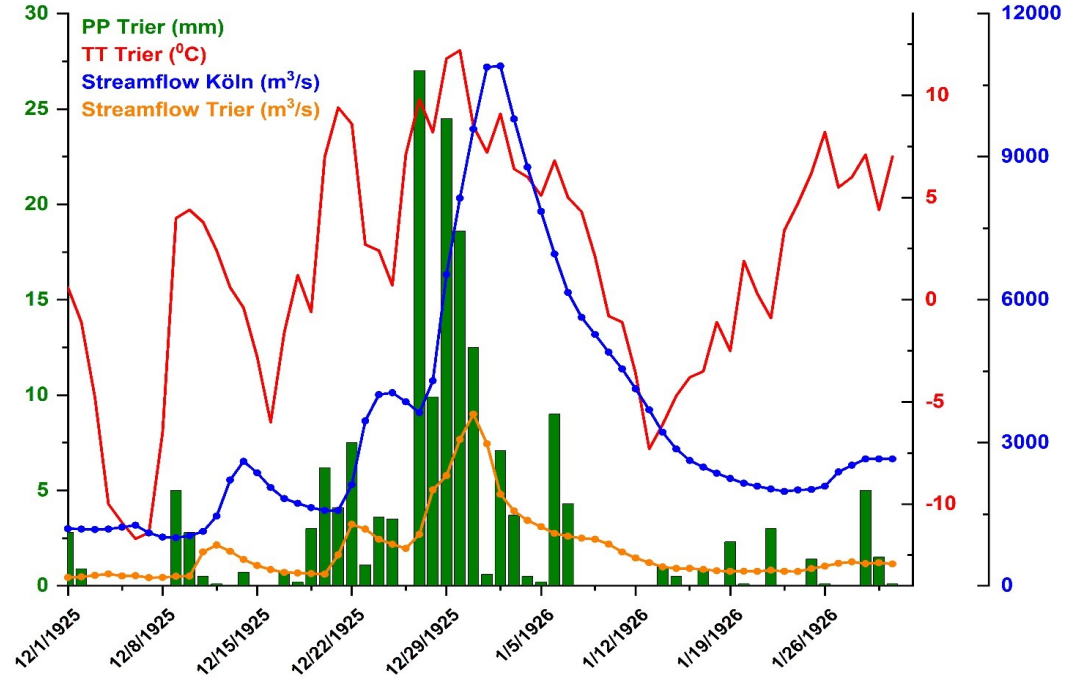

b)

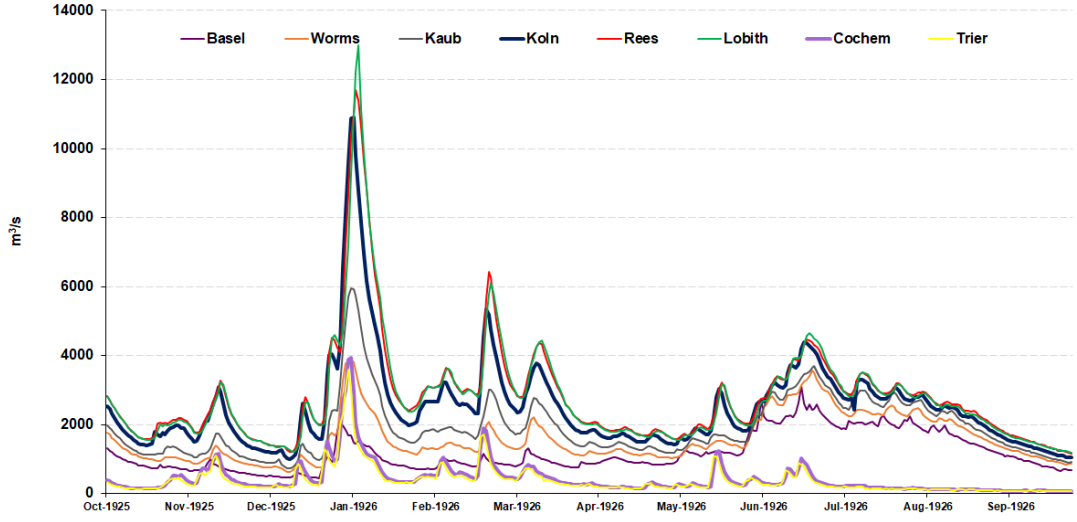

Figure 2. a) Daily precipitation (green bars) at Trier meteorological station, daily mean temperature (red line), daily streamflow at Köln gauging station (blue line) and daily streamflow at Trier gauging station (orange line) for the period 1.12.1925 – 31.1.1926 and b) Daily streamflow at different gauging station alone Rhine River (Basel, Worms, Kaub, Köln, Rees, Lobith) and Moselle River (Trier and Cochem) for the period 1.10.1925 – 30.09.1926.

https://doi.org/10.5194/hess-2020-149
Preprint. Discussion started: 14 April 2020

Hydrology and Earth System Sciences
Discussions
Open Access
EGU

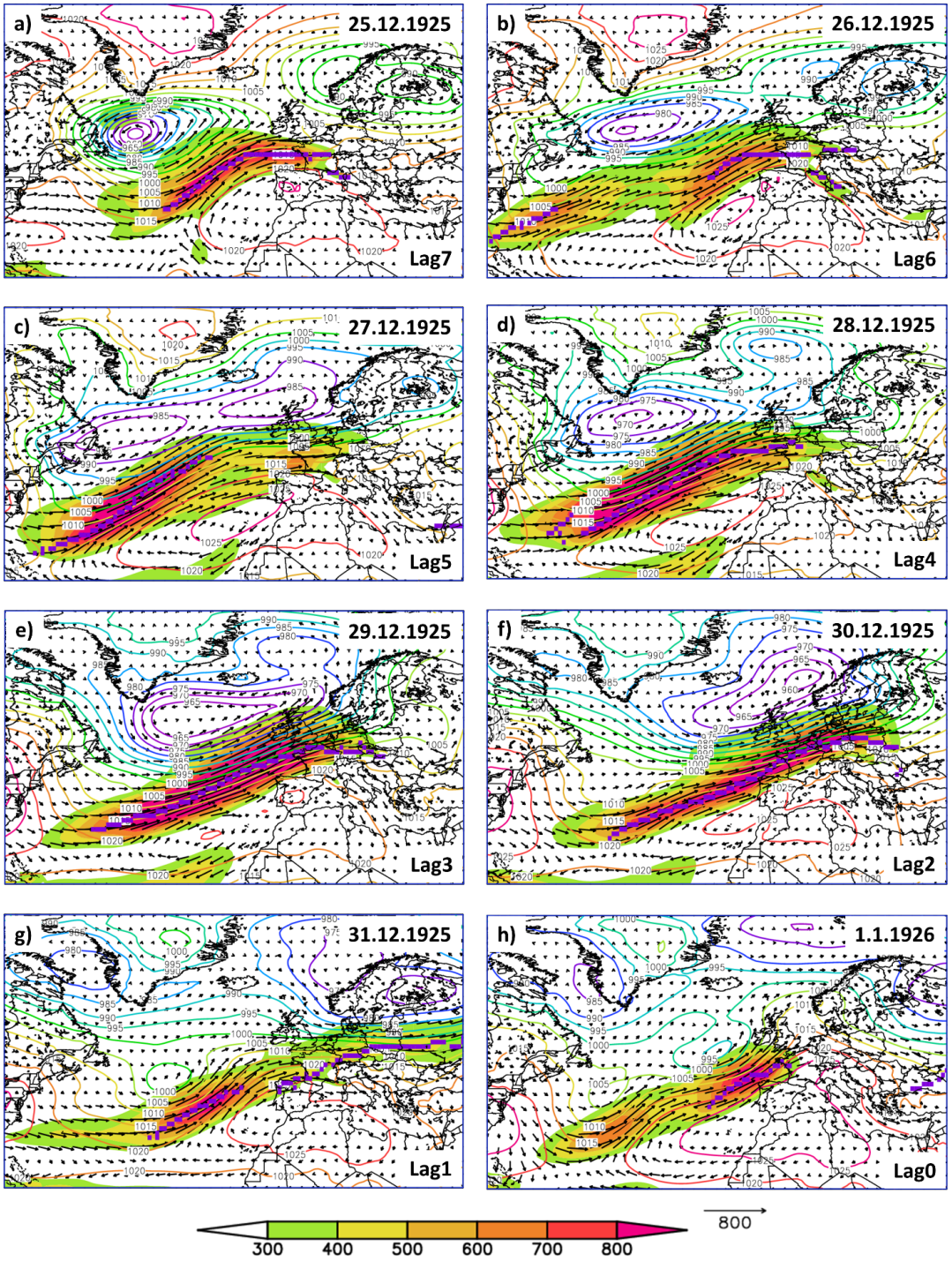

Figure 3. Daily sea level pressure (colored contour lines), magnitude of the integrated water vapor transport (shaded colors), direction of the integrated water vapor transport (vectors) and location of the AR axis (magenta line) for different time lags (0 – 7 days) for the 1925/26 flood event.

https://doi.org/10.5194/hess-2020-149
Preprint. Discussion started: 14 April 2020

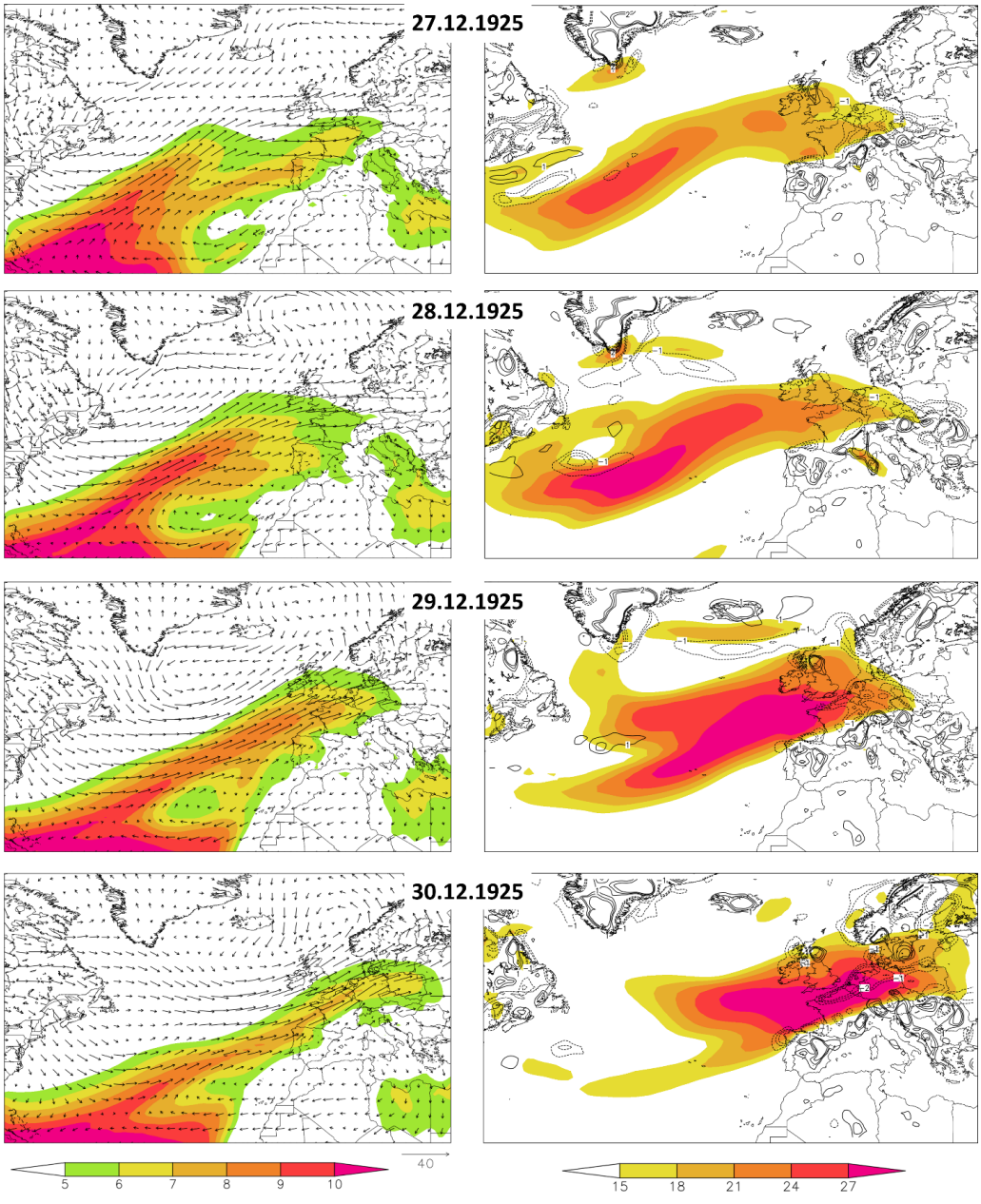

Figure 4. Left column - Daily specific humidity (shaded colors) and the wind direction (vectors) at 900 hPa level and Right column – zonal wind at 900 hPa level (shaded colors) and divergence/convergence (contour lines) for the days with rainfall events prior to the flood of 1925/26, at Trier station.

660

https://doi.org/10.5194/hess-2020-149
Preprint. Discussion started: 14 April 2020

Hydrology and Earth System Sciences
Discussions

a)

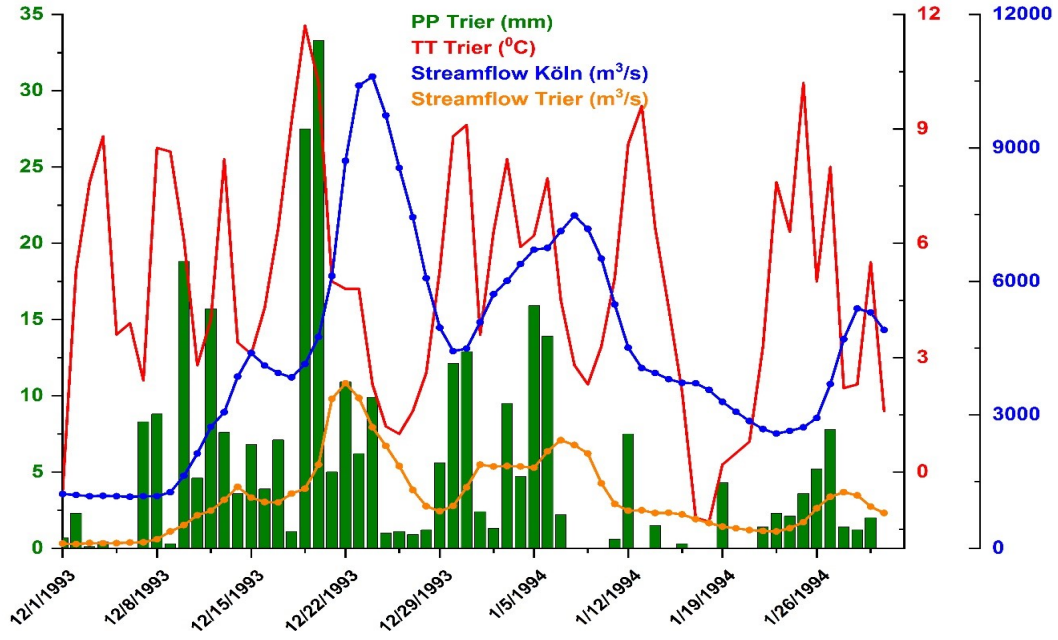

b)

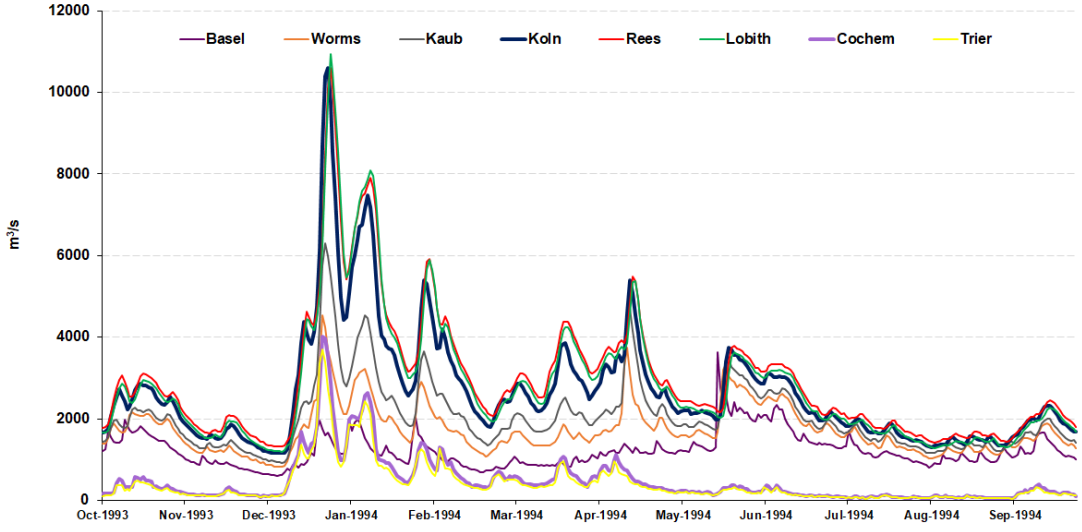

Figure 5. a) Daily precipitation (green bars) at Trier meteorological station, daily mean temperature (red line), daily streamflow at Köln gauging station (blue line) and daily streamflow at Trier gauging station (orange line) for the period 1.12.1993 – 31.1.1993 and b) Daily streamflow at different gauging station alone Rhine River (Basel, Worms, Kaub, Köln, Rees, Lobith) and Moselle River (Trier and Cochem) for the period 1.10.1993 – 30.09.1994.

665

https://doi.org/10.5194/hess-2020-149
Preprint. Discussion started: 14 April 2020

Hydrology and Earth System Sciences
Discussions
Open Access
EGU

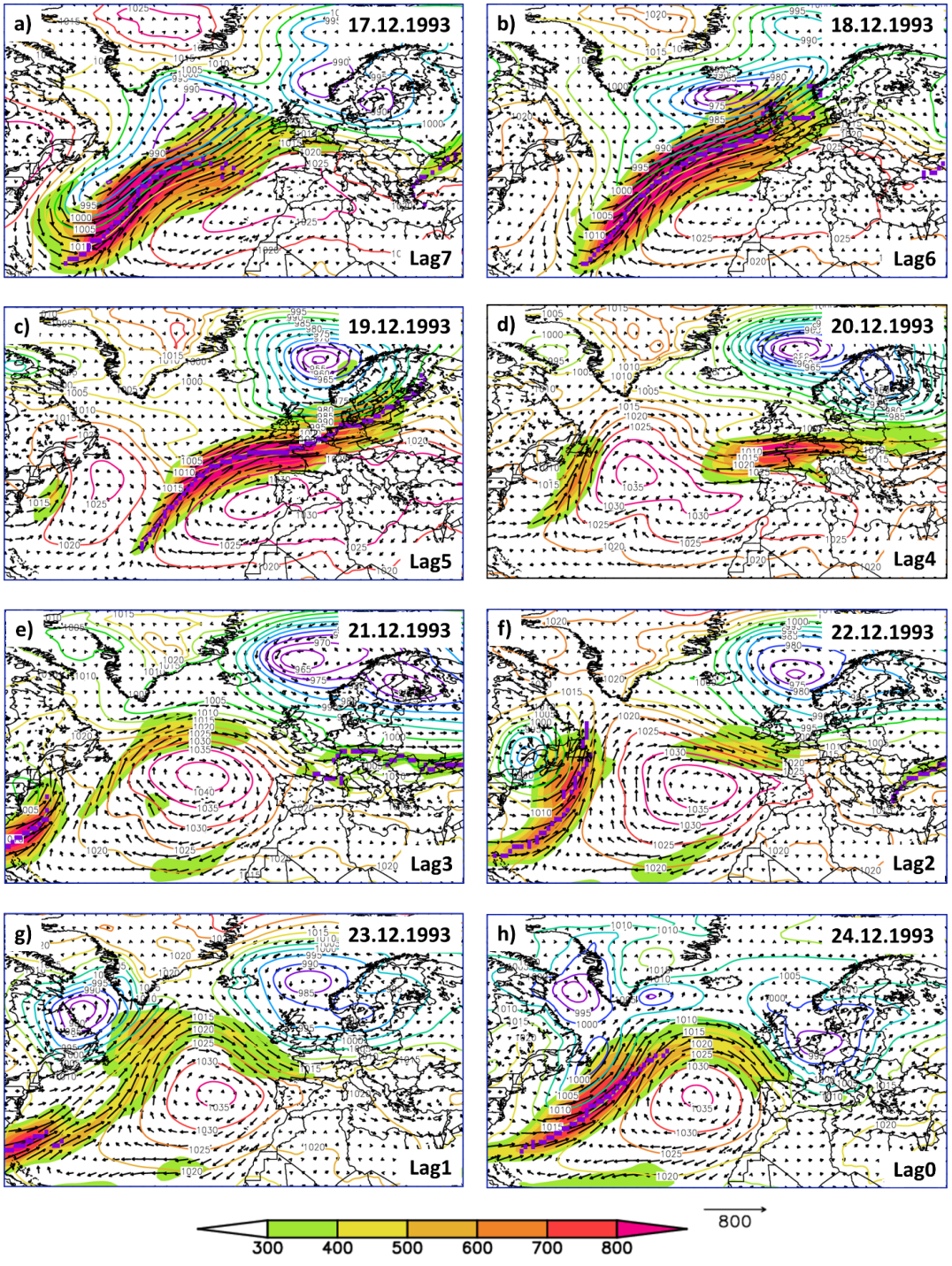

Figure 6. Daily sea level pressure (colored contour lines), magnitude of the integrated water vapor transport (shaded colors), direction of the integrated water vapor transport (vectors) and location of the AR axis (magenta line) for different time lags (0 – 7 days) for the 1993 flood event.

https://doi.org/10.5194/hess-2020-149
Preprint. Discussion started: 14 April 2020

Hydrology and Earth System Sciences
Discussions
Open Access
EGU

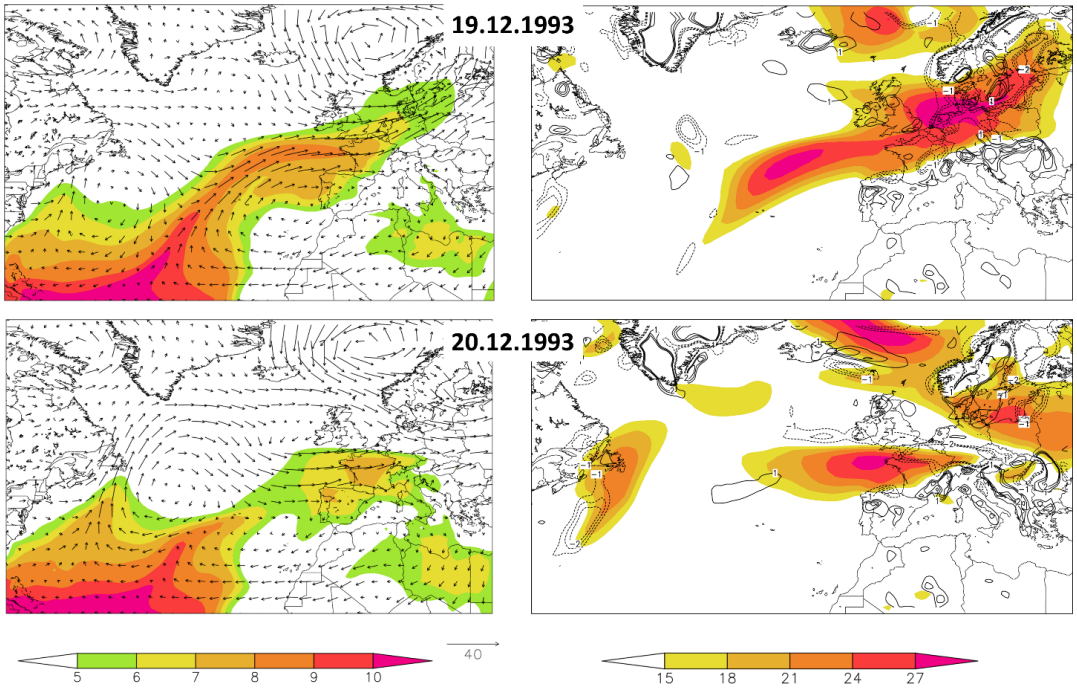

Figure 7. Left column - Daily specific humidity (shaded colors) and the wind direction (vectors) at 900 hPa level and Right column – zonal wind at 900 hPa level (shaded colors) and divergence/convergence (contour lines) for the days with rainfall events prior to the flood of 1993, at Trier station.

https://doi.org/10.5194/hess-2020-149
Preprint. Discussion started: 14 April 2020

Hydrology and Earth System Sciences
Discussions

a)

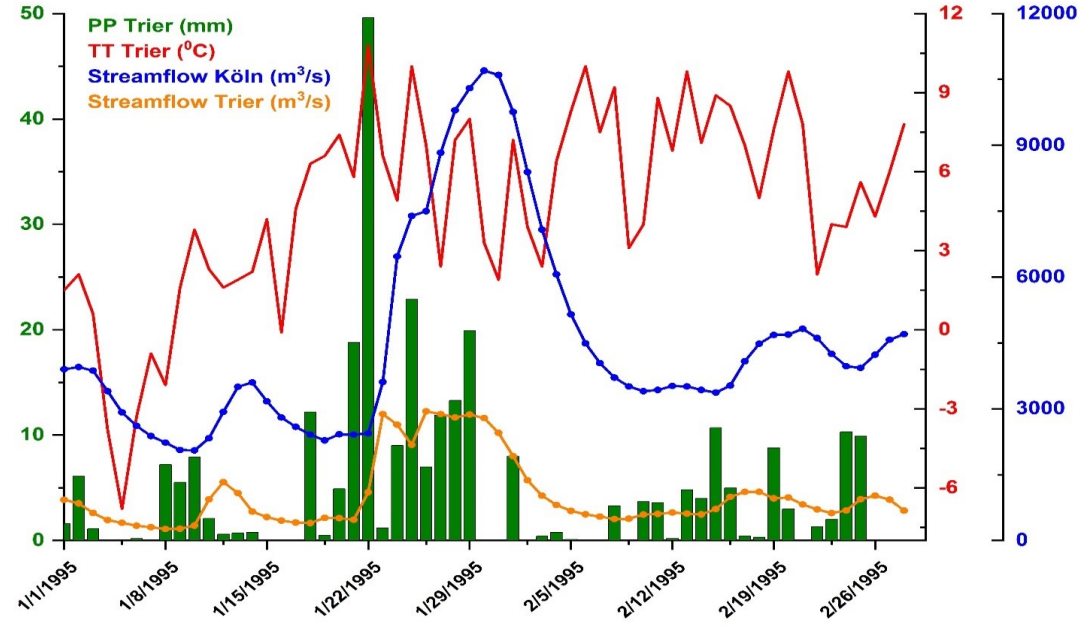

b)

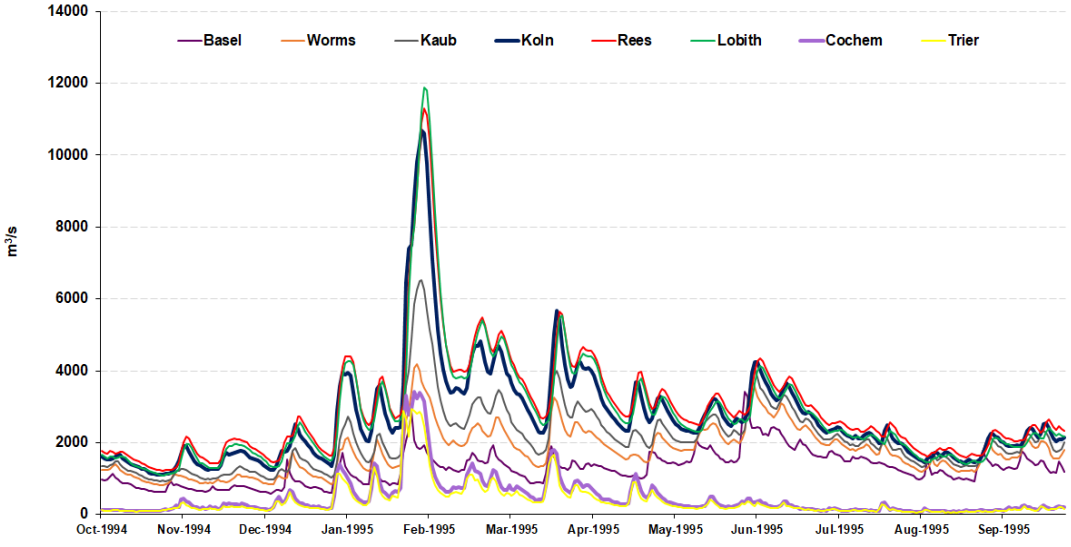

Figure 8. a) Daily precipitation (green bars) at Trier meteorological station, daily mean temperature (red line), daily streamflow at Köln gauging station (blue line) and daily streamflow at Trier gauging station (orange line) for the period 1.1.1995 – 28.2.1995 and b) Daily streamflow at different gauging station alone Rhine River (Basel, Worms, Kaub, Köln, Rees, Lobith) and Moselle River (Trier and Cochem) for the period 1.10.1994 – 30.09.1995.

https://doi.org/10.5194/hess-2020-149
Preprint. Discussion started: 14 April 2020

Hydrology and Earth System Sciences
Discussions
Open Access
EGU

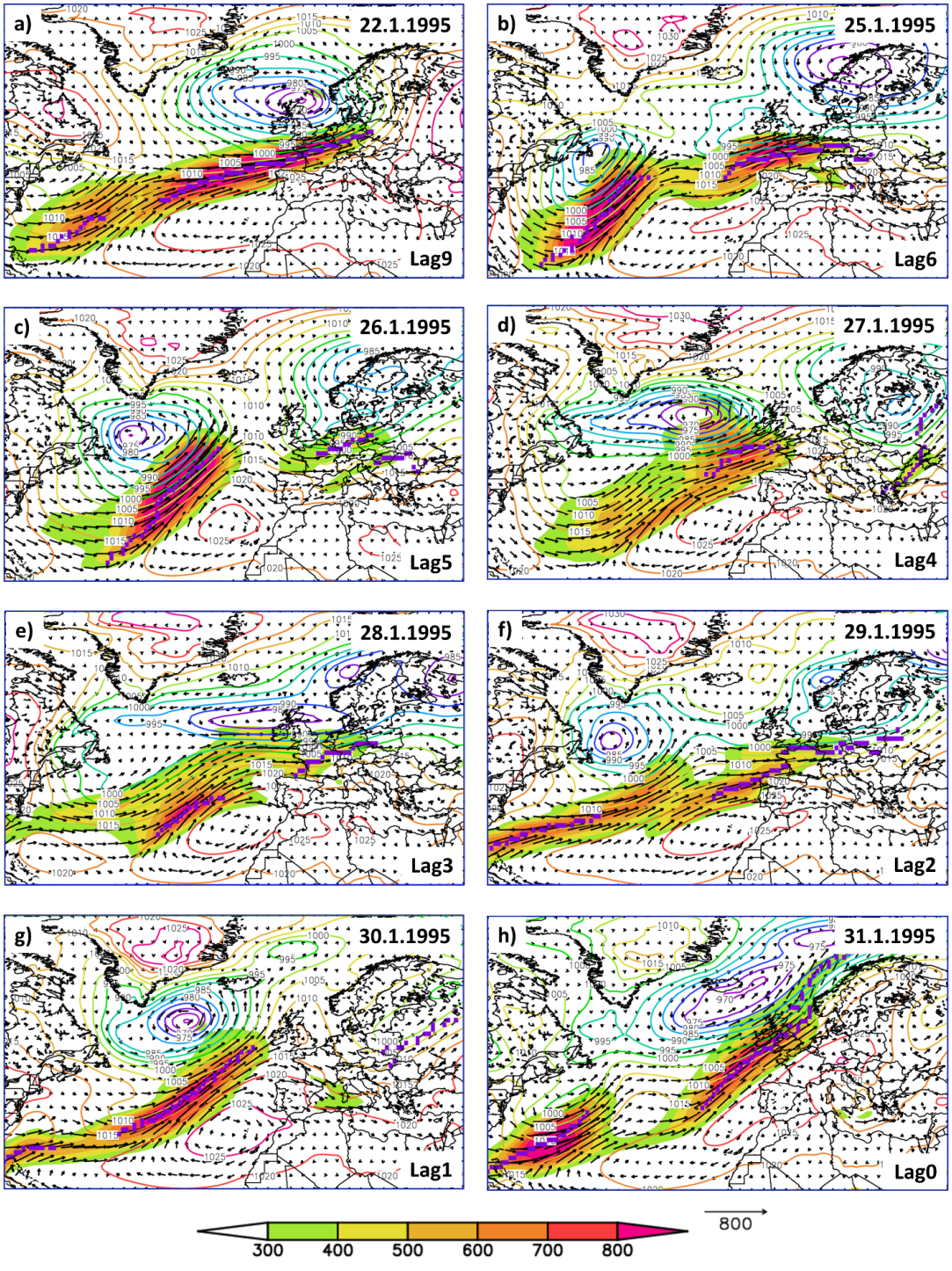

Figure 9. Daily sea level pressure (colored contour lines), magnitude of the integrated water vapor transport (shaded colors), direction of the integrated water vapor transport (vectors) and location of the AR axis (magenta line) for different time lags (0 – 7 days) for the 1995 flood event.

https://doi.org/10.5194/hess-2020-149
Preprint. Discussion started: 14 April 2020

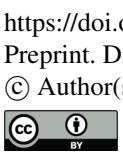

Hydrology and Earth System Sciences
Discussions
Open Access
EGU

695

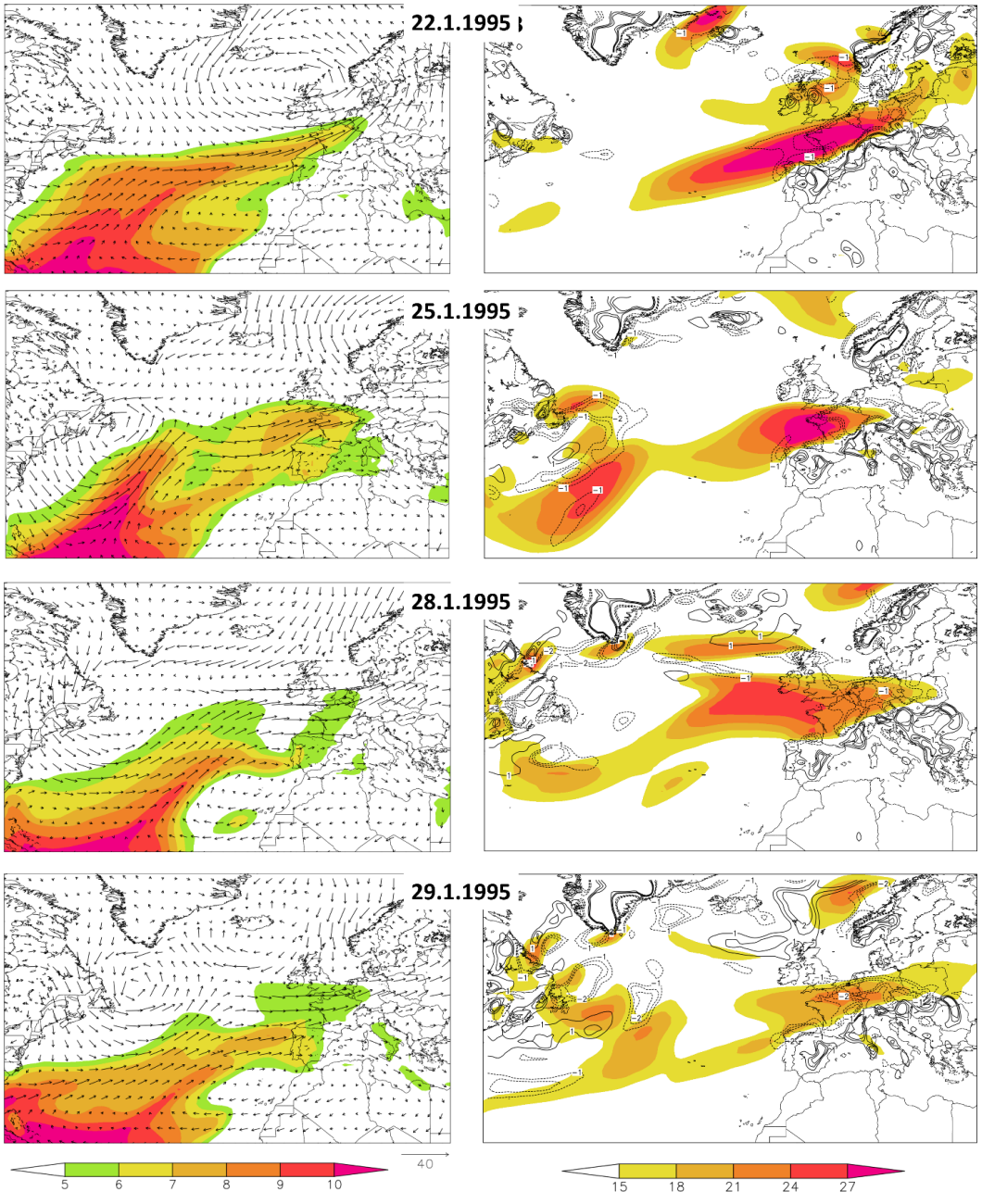

Figure 10. Left column - Daily specific humidity (shaded colors) and the wind direction (vectors) at 900 hPa level and Right column – zonal wind at 900 hPa level (shaded colors) and divergence/convergence (contour lines) for the days with rainfall events prior to the flood of January 1995, at Trier station.

https://doi.org/10.5194/hess-2020-149
Preprint. Discussion started: 14 April 2020

Hydrology and Earth System Sciences
Discussions
Open Access
EGU

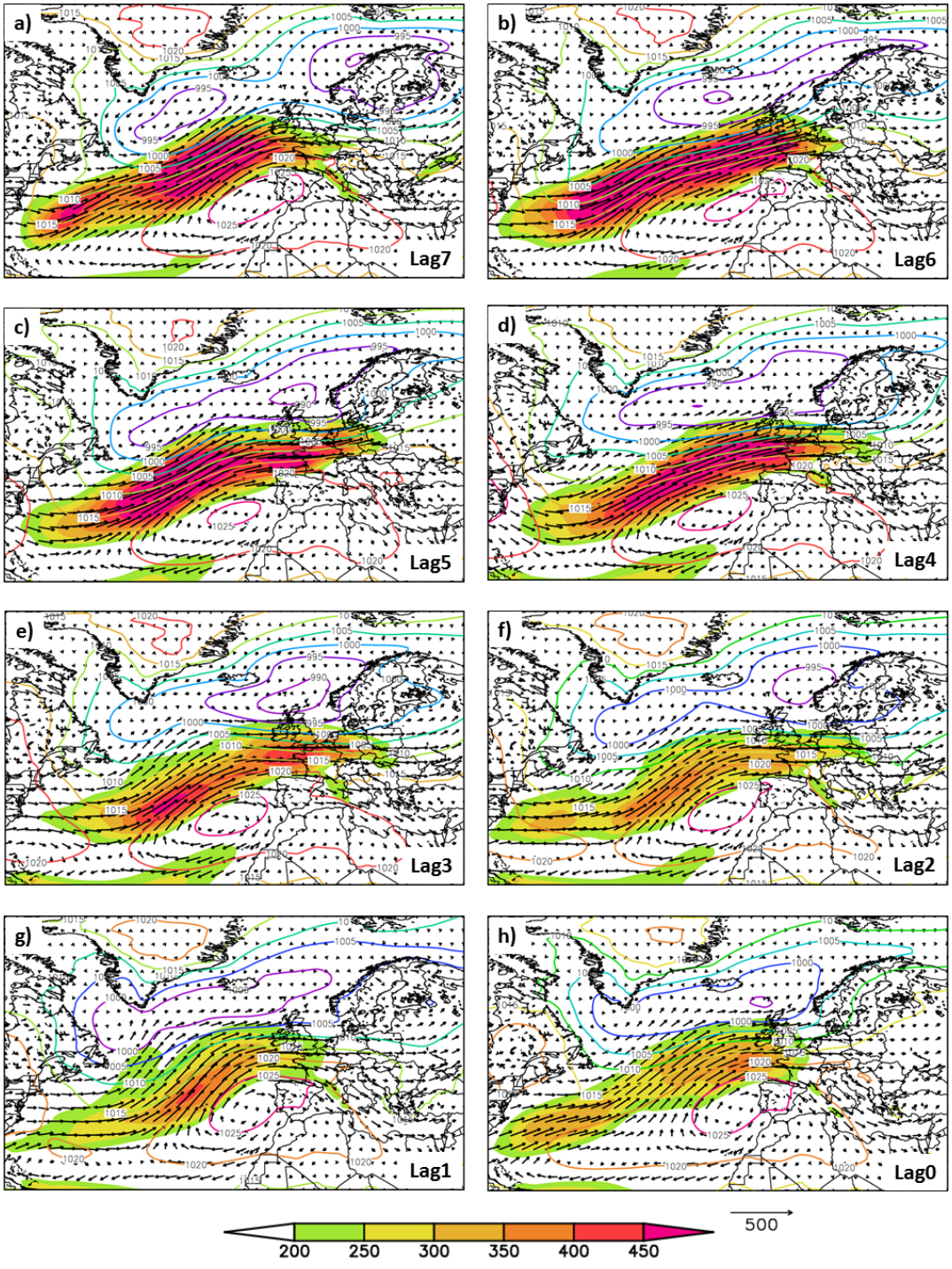

Figure 11. Composite of the mean sea level pressure (colored contour lines), magnitude of the integrated water vapor transport (shaded colors) and the direction of the integrated water vapor transport (vectors) for different time lags (0 – 7 days) for the 10 highest flood peaks recorded at Köln gauging station (see Table 1).

700

https://doi.org/10.5194/hess-2020-149
Preprint. Discussion started: 14 April 2020

Hydrology and Earth System Sciences
Discussions
Open Access
EGU

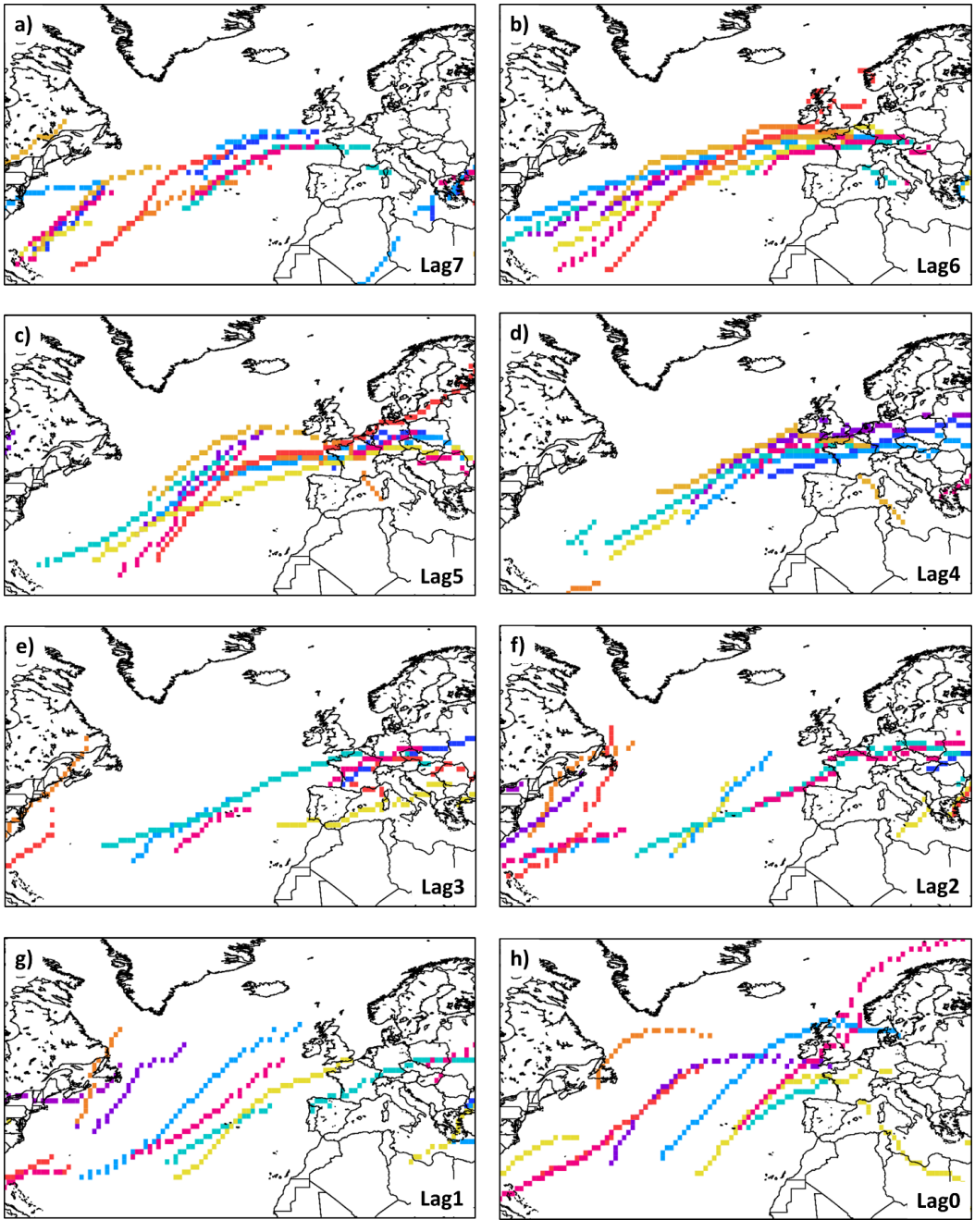

Figure 12. The AR axis location for the top 10 winter floods with different time lags (0 – 7 days). Each color is assigned to a flood peak.